



Cairo University
Egyptian Informatics Journal

www.elsevier.com/locate/eij
www.sciencedirect.com



FULL-LENGTH ARTICLE

Improved multiscale matched filter for retina vessel segmentation using PSO algorithm



K.S. Sreejini *, V.K. Govindan

Department of Computer Science, National Institute of Technology, Calicut, Kerala, India

Received 9 October 2014; accepted 13 June 2015

Available online 19 August 2015

KEYWORDS

Multiscale matched filter;
Optimization;
Retina vessels;
PSO

Abstract The concept of matched filter is widely used in the area of retina vessel segmentation. Multiscale matched filters have superior performance over single scale filters. The proposed approach makes use of the improved noise suppression features of multiscale filters. A major performance issue here is the determination of the right parameter values of the filter. The approach employs particle swarm optimization for finding the optimal filter parameters of the multiscale Gaussian matched filter for achieving improved accuracy of retina vessel segmentation. The proposed approach is tested on DRIVE and STARE retina database and obtained better results when compared to other available retina vessel segmentation algorithms.

© 2015 Production and hosting by Elsevier B.V. on behalf of Faculty of Computers and Information, Cairo University. This is an open access article under the CC BY-NC-ND license (<http://creativecommons.org/licenses/by-nc-nd/4.0/>).

1. Introduction

Automatic analysis of photographs of ocular fundus image of the retina along with the study of alternations in the blood vessels network can reveal the important features for the study, diagnosis and treatment of various diseases such as hypertension [1], diabetic retinopathy (DR) [2], diabetic macular edema (DME) [2–6], vessel occlusion [7] and various cardiovascular diseases [8]. Lesions, geometrical and morphological changes in blood vessels are the various features used. Geometrical and morphological changes include the changes in diameter

of vessels, curvature, tortuosity and appearance of vessels. DR creates new blood vessels and branches. Various lesions are symptoms of DR and DME. Hypertension reduces arteries leading to abnormal artery to vein width ratio (AVR). Vessel occlusion makes vessels longer. Thus, retina vessel segmentation is an important step in most of the algorithms for locating other retinal structures such as optic disk and fovea and serves as an aid for registration of images taken at different instants or at different locations of the retina. These registered images are useful in automatically monitoring the progression of certain diseases. Knowledge about vascular structure will reduce the false positive in lesion detection. Detection of vessels bifurcation and crossover points aids physicians in better diagnosis.

There are mainly two types of retina photography [3–5]: Fluorescein angiography (FA) and to use color fundus camera. In FA, images of vessel boundary edges are clearly defined than latter one but FA had side effects and is complicated. Most existing algorithms assume that image of retina is healthy, lesion and noise free. They show poor performance

* Corresponding author.

Peer review under responsibility of Faculty of Computers and Information, Cairo University.



Production and hosting by Elsevier

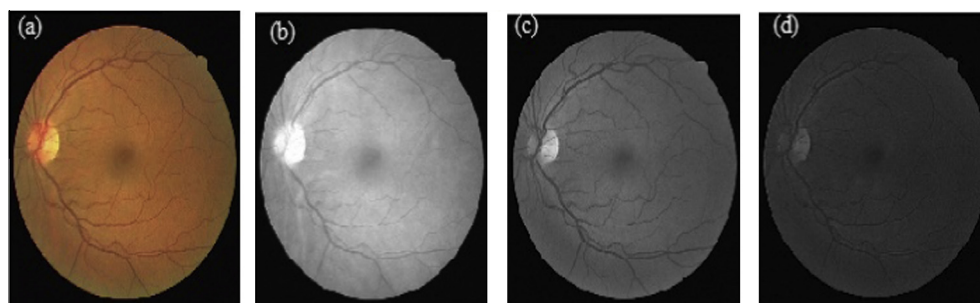


Figure 1 (a) Color retina image, [9], (b) red channel, (c) green channel and (d) blue channel.

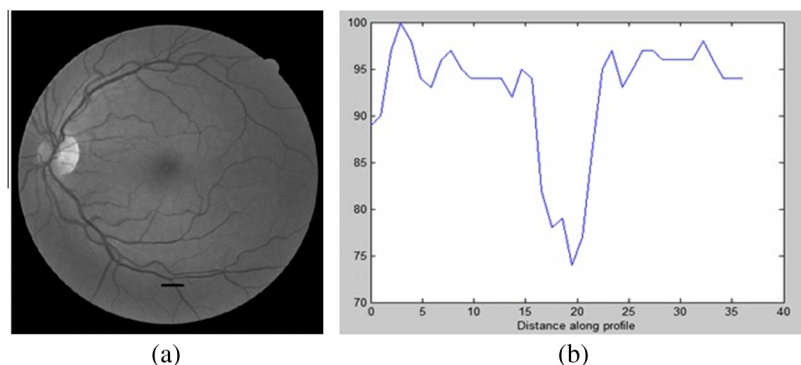


Figure 2 (a) Green band of colored retina image “01_test.tif” from DRIVE database, here vessel cross section is marked, (b) gray level intensity profile of marked region in 1(b).

in case of abnormal retina images and depend upon different parameter configurations. Manual segmentation is tedious and expensive. Thus automatic algorithms that do not depend on parameter configuration with reduced cost are needed to screen larger populations of vessel abnormalities.

Fig. 1 shows a colored retina image from DRIVE database [9] and the red, green and blue channels of the same image. Vessels are clearer in green channel of the image than other channels, and hence this channel is used for analysis. In Fig. 2a, green channel of the image is chosen and one cross section of the vessel is marked with a dark line. Gray level intensity profile along a line in the cross section is shown in Fig. 2b. Its shape is similar to the Gaussian curve.

2. Related works

Several approaches are available for blood vessel segmentation. These can be mainly classified as based on: edges, mathematical morphology, trace, machine learning and matched filter.

Edge based methods find the vessel edges with an edge detector such as Sobel, Canny and Prewit operators [10]. These approaches work properly on distinct and sharp edges only. The literature demonstrates that such edge based methods are not suitable for accurate retina vessel segmentation.

In mathematical morphology methods, first we get prior known vasculature shape features, and then vasculature is filtered from the background for segmentation. Zana and Klein [11] combined morphological filters along with cross curvature evaluation to separate the vessels from retina images.

Use of bit planes with vessel central lines to extract retina vasculature is discussed in [12]. The approach requires more processing time.

Trace-based methods [13] map out the global network of blood vessels after edge detection by tracing out the center lines of vessels. Such methods rely heavily on the result of edge detection and need longer processing time.

Machine-Learning based methods [14,15] are divided into two subgroups: supervised methods [14] and unsupervised methods [15]. Supervised methods exploit some prior labeling information to decide whether a pixel belongs to a vessel or not, while unsupervised methods do the vessel segmentation without any prior labeling knowledge. Supervised methods require pre-labeled training datasets and efficient training time and need ground truth segmentation for training which is not available in real time applications.

Supervised ridge-based vessel detection method is proposed in [14] by Staal et al. The approach is based on the extraction of ridges, which coincide approximately with the vessel center lines. These ridges are used as primitives to form line elements. Each pixel was then assigned to its nearest line element, the image thus being partitioned into patches. For every pixel, 27 features were firstly computed and those obtaining the best class reparability were finally selected. Feature vectors were classified by using a k-NN classifier, and a sequential forward feature selection was employed.

Early methods of vessel segmentation were based on matched filtering [16]. It is based on the assumption that intensity profile along a cross section of a vessel has the shape of Gaussian. A set of 12 Gaussian shaped filters are used to match the vessels at different directions. For each pixel, the

maximum response is retained. The drawback is that its response is high for non-vessels too, which results in increased false positives.

Later, many extensions of matched filter are used, such as matched filter (MF) combined with pulse coupled neural networks as discussed in [17]. Otsu algorithm [18] is used to obtain segmentation results. Improvement of the matched filter response by Ant colony algorithm is proposed in [19]. Zero mean Gaussian matched filter with first order derivative of Gaussian filter is proposed in [20]. MF has high response for true vessels and non-vessel but the local mean of its response to the First-order Derivative of Gaussian (FDOG) will also be high. Scale selection of matched filter is very important. Empirical estimation of scale selection is done by Chaudhuri et al. [16], simple optimization is done by Al-Rawi et al. [21], and genetic algorithm based optimization is performed in [22].

In [23], a new kernel function, Cauchy PDF is used as a substitute for Gaussian kernel for segmentation and authors found filter parameters by trial and error method.

Usually vessel width is varying across the retina fundus images from 15 pixels (very large vessels) to 3 pixels (small vessels) [24]. Thus, simultaneous detection of vessels of different width is very difficult. Li et al. [24] claim that the performance of multiscale matched filter is better than single scale approach. The response of multiscale filters depends upon the selection of scales of the filters. However, the selection of the right values of parameters of multiscale matched filter is a difficult task for achieving good results.

The main problems in vessel segmentation are poor quality images, local intensity contrast of vessels and variations in the width of the vessels. Small vessels are overwhelmed by different noises like Gaussian. This makes the accurate segmentation a challenging problem. This paper proposes to employ multiscale filter for vessel segmentation, and to address the parameter value selection problem in multiscale matched filters.

Organization of rest of this paper is as follows: Section 3 presents a brief introduction about the retina database used, matched filter, multiscale matched filter and basic particle swarm optimization. The implementation details of PSO based multiscale Gaussian matched filter are described in Section 4. Experimental results of the proposed method on image datasets and discussions are given in Section 5, and finally the paper is concluded in Section 6.

3. Background

3.1. Image database

3.1.1. DRIVE

In this work, we used the retina fundus images from the Digital Retinal Images for Vessel Extraction (DRIVE) database [9], introduced in 2004. Database contains 40 retina images; 20 train and 20 test images, captured by Canon CR5 non-mydratic 3CCD camera at 45° field of view (FOV). The images have a size of 768 × 584 pixels, eight bits per color channel. This contains normal and abnormal images and hand labeled images for each image provided by experts to evaluate the performance of the proposed method. The database also includes masks to separate the FOV from the rest of the image. Two sets of manual hand labeled images are available. The

first manual offers hand labeled images for all the images in the dataset, while the second manual offers hand labeled images for just half of the images. First, hand labeled images is used as ground truth to evaluate the results of segmentation.

3.1.2. STARE

STructured Analysis of the RETina (STARE), is an another public database that provides retina color fundus image [14]. The dataset consists of 20 color images : 10 normal and 10 abnormal, captured by a TopCon TRV-50 fundus camera at FOV of 35° and image size of 700 × 605 pixels. The dataset also provides ground truth for blood vessels in two sets of hand labeled images performed by two observers. The second hand labeling set in STARE is taken as second observer, while the first set is used as ground truth.

3.2. Matched filter

Matched filter (MF) is the most widely used template matching algorithm for retina vessel segmentation. It was first proposed by Chaudhuri et al. [16]. Here, we used the prior assumption that the cross section of the vessels can be approximated by a Gaussian function.

The Gaussian MF is defined as

$$k(x, y) = -\exp(-x^2/2\sigma^2) \quad \forall |y| \leq L/2 \quad (1)$$

σ is the scale of the filter.

L is the length of the vessel segment directed in one direction which is assumed as piecewise linear.

Kernel, $k(x, y)$ is rotated in different orientations to detect the vessels in different orientations and (x, y) is the coordinate of each element in kernel. Maximum response from the filter bank is used. i.e., when both kernel and the vessel are in same direction response is maximum. Here, rotating by an amount of 15° results a filter bank with 12 kernels.

The neighbourhood N is defined as

$$N = \{(u, v), |u| \leq T, |v| \leq L/2\} \quad (2)$$

T is the position where Gaussian curve should be cut, usually its value set as $3 * \sigma$. p_i be the points in the neighbourhood.

$$p_i = [u \quad v] = [x \quad y] \begin{bmatrix} \cos \theta & -\sin \theta \\ \sin \theta & \cos \theta \end{bmatrix} \quad (3)$$

θ – angle in which the kernel is rotated.

$[u \quad v]$ – new coordinates resulted from rotating $[x \quad y]$.

$\begin{bmatrix} \cos \theta & -\sin \theta \\ \sin \theta & \cos \theta \end{bmatrix}$ – rotation translation matrix.

Then weights in the corresponding rotated kernel are given by

$$k_i(x, y) = -\exp(-u^2/2\sigma^2) \quad \forall p_i \in N \quad (4)$$

The mean of the filter is set to 0 for removing smooth background.

The filter has only a few filter parameters to adjust to achieve good performance for every application. Though the technique is very simple, it responds not only to vessels but to non-vessels too. As it is a commonly used useful approach, improving its performance is highly desirable.

3.3. Multiscale matched filter

In grayscale retina images, usually thin vessels are unclear and hence most methods available in the literature fail to detect vessels properly. This paper proposes multiscale filter for vessel detection.

The filter response of a matched filter $m_i(x, y)$ to an input image $f(x, y)$ can be expressed by

$$r_i(x, y) = m_i(x, y) * f(x, y) \quad (5)$$

Scale production of two filters with different scales

$$P_i(x, y) = r_i(x, y) \cdot r_j(x, y) \quad (6)$$

In this work, we proposed a new optimization method to find the matched filter parameters to increase the performance of the matched filter, i.e., to find better filter parameter values for L , σ and T . Direct estimation of parameters will not result in good detection. Empirical estimation is done by Chaudhari et al. [16], simple optimization is done by Al-Rawi et al. [21] and genetic algorithm based optimization is performed in [22]. Here, we used PSO optimization technique and better performance is achieved. Matched filter with two scales is used. Large values of scale are used to detect big vessels and small values are used to detect small vessels.

3.4. Particle swarm optimization

Swarm intelligence based optimization algorithm was introduced by Kennedy and Eberhart [25] in 1995. The algorithm mimics the social behaviour of fish schooling or flock of birds known as swarm. Particles mean individual swarm members which is a solution. Every particle has fitness depends upon the problem to be solved. At first, optimal fitness value is not known by any particle. The algorithm operates iteration

by iteration and output in each iteration is compared with local best and global best. Global best solution of a particle, gbest is computed with swarm and local best of a particle, pbest is computed by self. In every iteration position and velocities are updated by (7) and (8) and are repeated until some convergence criterion is met. Convergence criterion also depends on the problem.

$$v_i(t+1) = wv_i(t) + c_1r_1[pbest - x_i(t)] + c_2r_2[gbest - x_i(t)] \quad (7)$$

$$x_i(t+1) = x_i(t) + v_i(t+1) \quad (8)$$

i is the index of the particle.

t represents the iteration.

v_i is the velocity of the particle at time t .

x_i is the position of the particle at time t

W is called inertial weight, reduced to minimum value in different iteration

c_1 and c_2 are the learning factor for controlling the particle movement in an iteration ranges from 0 ~ 2.

r_1 and r_2 are random numbers valued between 0 and 1.

pbest, solution found by an individual particle.

gbest, the fittest particle found by swarm.

Table 1 Results of proposed method on DRIVE database.

Type of filter	Parameters	Sen.	Spec.	Acc.
Single scale	$L_1 = 1, \sigma_1 = 3, T_1 = 6$	34.10	99.81	94.25
	$L_2 = 2, \sigma_2 = 6, T_2 = 6$	77.70	95.21	93.71
Multiscale	$L_1 = 1, \sigma_1 = 3, T_1 = 6$ and $L_2 = 2, \sigma_2 = 6, T_2 = 6$	71.32	98.66	96.33

Note: Sen. denotes sensitivity in (%), Spec. denotes specificity in (%), and Acc. denotes accuracy in (%).

Table 2 Results of proposed method on STARE database.

Img. No.	Sensitivity (%)	Specificity (%)	Accuracy (%)
1	65.43	96.72	94.22
2	53.85	97.01	94.14
3	79.04	93.16	92.31
4	32.45	99.69	94.70
5	76.78	94.72	93.10
44	82.76	93.54	92.79
77	85.03	95.22	94.40
81	84.85	96.19	95.34
82	83.27	96.48	95.44
139	78.17	95.20	93.83
162	85.35	96.59	95.79
163	89.35	96.64	96.07
235	78.54	96.80	95.17
236	79.23	97.05	95.44
239	72.02	97.71	95.49
240	54.96	99.04	94.54
255	78.54	98.23	96.47
291	58.65	99.64	97.56
319	56.85	99.21	97.39
324	59.23	98.49	95.87
Avg.	71.72	96.87	95.00

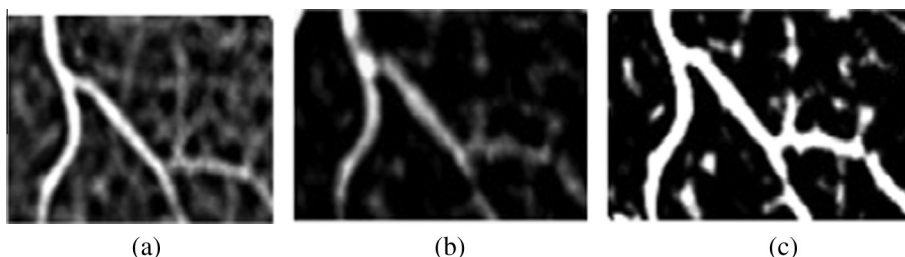


Figure 3 (a) and (b) Matched filter responses at different scales, (c) is the scale production of (a) and (b).

4. Proposed method

The proposed approach makes use of multiscale filter described in the previous section for segmentation of retina vasculature to detect vessels. PSO is employed for computing the parameters of multiscale filter. The images in the database are used for determining the optimal values of parameters.

4.1. Optimization of multiscale matched filter

In this work particle swarm optimization is used to find the optimized matched filter parameters for L , σ and T . Here, matched filter with two scales is used. The search space is not very large and green band of the retina image after median

filtering is used. The ranges of values used for different parameters of the filter in the optimization process are as follows:

$L_1 = \{1, 2, \dots, 10\}$, $\sigma_1 = \{1, 2, \dots, 10\}$, $T_1 = \{1, 2, \dots, 10\}$ and $L_2 = \{1, 2, \dots, 10\}$, $\sigma_2 = \{1, 2, \dots, 10\}$, $T_2 = \{1, 2, \dots, 10\}$. Particle is a candidate solution consist a set of $\{L_1, \sigma_1$ and $T_1\}$ and $\{L_2, \sigma_2$ and $T_2\}$.

The algorithm is presented in the following:

Step 1: Initialization of swarm.

In this work, population = 30, inertial factor = 1.2, number of iteration = 50.

Step 2: Position and velocities of the particles are initialized. Here, the velocities of the particles are set to zero and positions are randomly set within the boundaries of search space.

Step 3: Loop

For each particle

1. Generate two matched filter kernel with different degrees of rotation.
2. Convolve the retinal input image with the generated matched filters.
3. Multiply the matched filter response to suppress noise and maximum response from matched filter responses is used.
4. Compute the area under receiver operating curve (ROC), which is used as the fitness function of the proposed method, of the segmented image.
5. Update each particle's velocity according to (7).
6. Update each particle's position according to (8).

end

Table 3 Performance comparison of proposed method with other existing method on STARE database.

Techniques	Sensitivity (%)	Specificity (%)	Accuracy (%)
Human observer	89.52	93.23	94.70
Fraz et al. [12]	73.11	96.80	94.42
Staal et al. [14]	–	–	95.16
Kande et al. [15]	–	–	89.76
Zhang et al. [20]	71.77	97.53	94.84
Hoover et al. [26]	67.51	95.67	92.67
Soares et al. [27]	–	–	94.80
You et al. [28]	72.60	97.56	94.97
Martinez-Perez et al. [29]	76.9	94.49	92.6
Proposed method	71.72	96.87	95.00

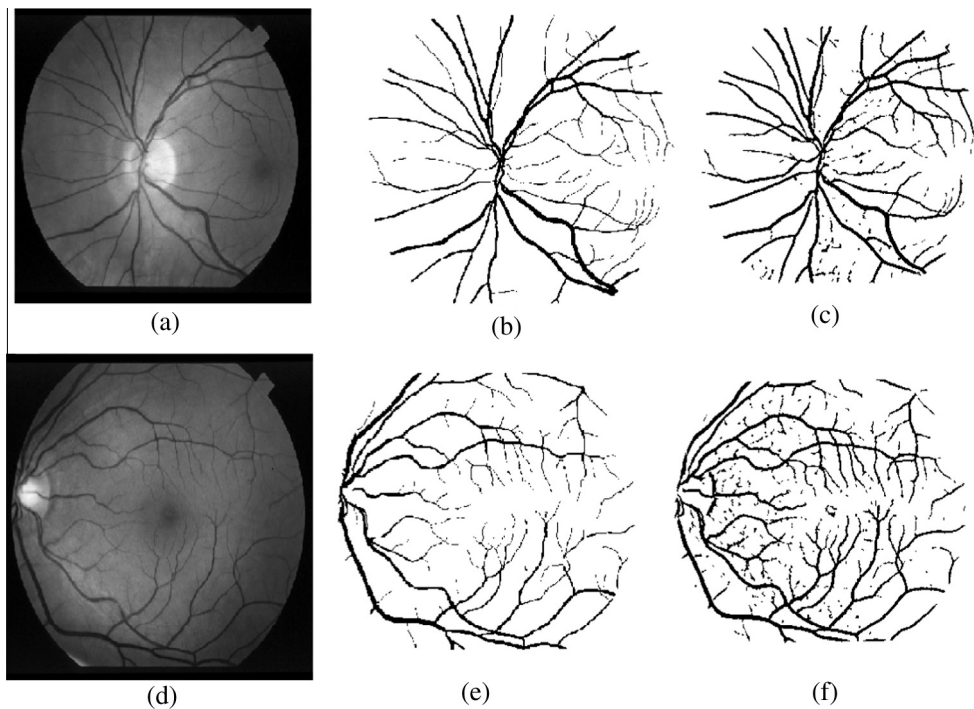


Figure 4 (a) and (d) Green channel of retina image from STARE database, (b) and (e) ground truth image, (c) and (f) the output of proposed method.

Until meets the stopping criteria (until t is the maximum of the iterative times, or the best solution remains the same).

Step 4: Return the selected optimal particle for generating output image.

Filtered output image is obtained by applying matched filter with parameters $\{L_1, \sigma_1 \text{ and } T_1\}$ and $\{L_2, \sigma_2 \text{ and } T_2\}$ to input fundus image f . This, filtered image is binarized with different threshold values range from 0 to 1 incrementing by 0.05. Several binary images are thus obtained as results of thresholding. The ground truth image provided by the database is used for computing performance of vessel detection.

True pixels – pixels present in detected image and ground truth.

False pixels – pixels present in detected image but not in ground truth.

True_ratio – Ratio of the number of true pixels to the number of vessel pixels in *ground truth*.

False_ratio – Ratio of the number of false pixels to the number of non-vessel pixels in *ground truth*.

The plot of the false ratio versus the true ratio provides the ROC, and the area under the ROC is used as the fitness function of this PSO optimization. The individual will be selected based on the highest area under the ROC. In the case of perfect detection, area under ROC will be one.

4.2. Vessel segmentation

4.2.1. Preprocessing

Green component of the input retina image is used as the blood vessels are clearer in this band of retina image than other bands.

Median filtering is applied to green band of the image, and this output is subtracted from the original green band of the retina image. Large filter window size, 30×30 is used.

4.2.2. Multiscale matched filter

Filtered output image is obtained by applying optimized matched filter with parameters $\{L_1, \sigma_1 \text{ and } T_1\}$ and $\{L_2, \sigma_2 \text{ and } T_2\}$ to input fundus image f . This filtered image is thresholded by using global thresholding [18].

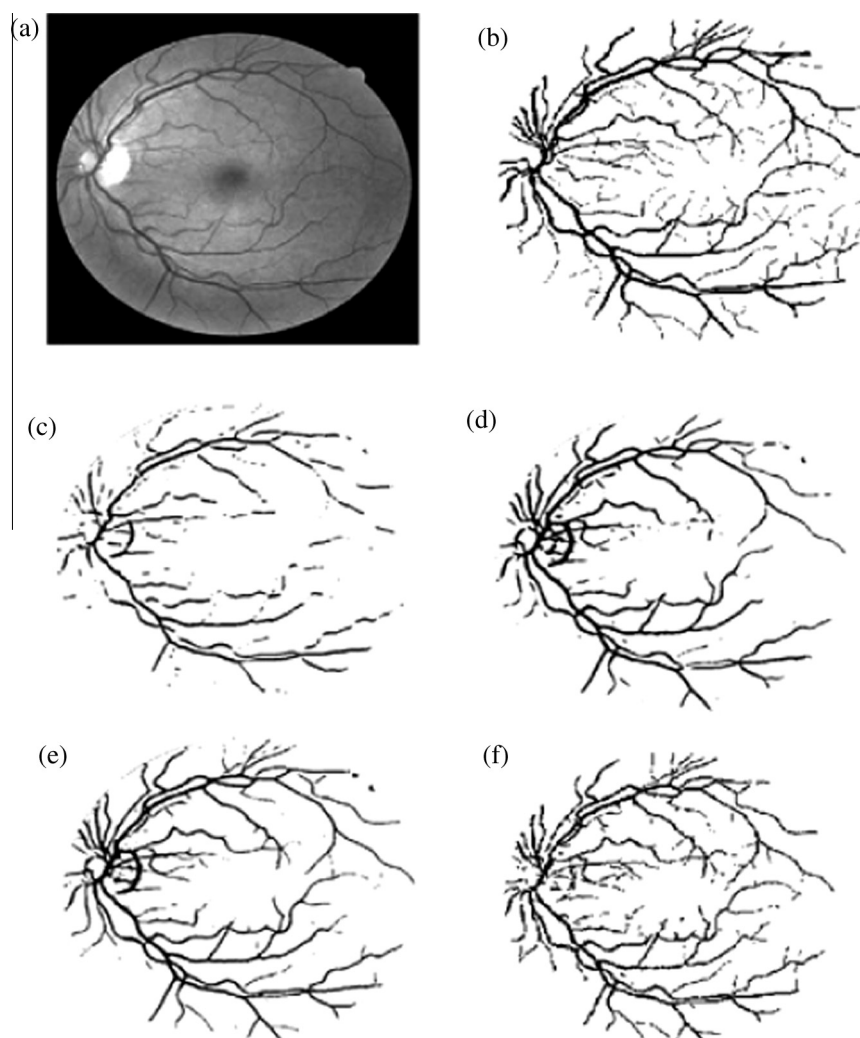


Figure 5 (a) The retinal image “01_test.tif” from the DRIVE retina database, (b) ground truth, (c) the output image using GMF with Chaudhuri et al. [16] parameters, (d) the output image using OGMF with Al-Rawi et al. [21] parameters, (e) the output image using GA optimization [22] and (f) the output of proposed method.

4.2.3. Fine segmentation

Background subtracted image is generated by median filter of large size. The pixels present in both background subtracted image and matched filter output image are taken as the actual output pixels. Small pixels are removed to avoid the false detection of vessels.

5. Results and discussion

We implemented the proposed method in MATLAB 7. 12. 0 and evaluated the performance of the improved Gaussian multiscale matched filter on DRIVE and STARE database. Best filter parameters are found by using the first image of the database as the input of the optimized matched filter. As PSO optimization involves different random operations, same output filter parameters may not be obtained even if we reinitialize and run the program again with the same parameters and inputs.

Terms used in performance metrics are

$$\text{sensitivity} = \frac{TP}{TP + FN} \quad (9)$$

$$\text{specificity} = \frac{TN}{TN + FP} \quad (10)$$

$$\text{accuracy} = \frac{TP + TN}{TP + TN + FP + FN} \quad (11)$$

5.1. Performance comparison of multiscale matched filter with single scale matched filter

The multiscale matched filter works better than single scale matched filter. The performance is demonstrated in Table 1. The overall performance metric is found to be better in multiscale matched filter. The first matched filter provides high specificity and accuracy but low sensitivity whereas the second provides low specificity and accuracy but high sensitivity. The multiscale matched filter that uses these two matched filters provides good sensitivity, specificity and accuracy as demonstrated in Table 1.

5.2. Performance of multiscale Matched filter in vessel segmentation

Chaudhuri et al. [16] selected the matched filter parameters, (L , σ , T) as (9, 2, 6). Al-Rawi et al. [21] proposed optimized Gaussian matched filter (OGMF) with parameters, (L , σ , T) as (10.8, 1.9, 8), and a two stage Gaussian matched filter (TSGMF) with parameters for first stage as (7.6, 1.9, 8) and second stage as (10.8, 1.9, 8). $L = 13.6947$, $\sigma = 0.4942$, and $T = 5.2275$ are the values found by using genetic algorithm for the optimization of Matched filter parameters in [19] and they used (13.4086, 0.5745, 6.2866) as (L , σ , T). Importance of scale production of multiscale matched filter is demonstrated in Fig. 3. Matched filter response with different scales and its production image are presented. We can observe that most of the noise is suppressed and maximum response is retained in (c). The proposed method chooses (1, 3, 6) and (2, 6, 6) as the matched filter parameter values for DRIVE database. For STARE database, the multiscale matched filter values chosen are (3, 2, 6) and (2, 3, 6).

Table 4 Performance comparison of proposed method with other existing method on DRIVE database.

Techniques	Sensitivity (%)	Specificity (%)	Accuracy (%)
Human observer	77.63	97.23	94.70
Zana and Klein [11]	69.71	93.77	89.84
Fraz et al. [12]	71.52	97.69	94.30
Staal et al. [14]	73.45	–	94.42
Kande et al. [15]	–	–	89.11
Chaudhuri et al.[16]	33.57	–	87.73
Cinsdikici and Aydin [19]	–	–	92.93
Zhang et al. [20]	71.20	97.24	93.82
Al-Rawi et al. [21]	–	–	95.35
Soares et al. [27]	–	–	94.66
Martinez-Perez et al. [29]	63.89	–	91.81
Perez et al.[30]	66.0	96.12	92.20
Martinez-Perez et al. [31]	72.46	96.55	93.44
Miri and Mahloojifar [32]	73.52	97.95	94.58
Proposed method	71.32	98.66	96.33

Table 2 demonstrates the average performance of figures-sensitivity, specificity and accuracy of the proposed vessel segmentation on DRIVE database. The performance comparison with many of the existing approaches presented in Table 3 demonstrates the overall superiority of the proposed approach (see Fig. 4).

Fig 5 shows the results of segmentation algorithm on first image of DRIVE retina image. Green channel of image is shown in (b) and outputs of Classical Gaussian matched filter are in Fig. 5(c), and filter improvement by Al-Rawi et al.[21] is shown in Fig. 5(d), GA optimization [22] output is shown in Fig. 5(e) and the output of proposed method is shown in Fig. 5(f). From Fig. 5, we can observe that Chaudhari et al. [16] fail to detect small vessels and false detection near to optic disk is more in (d) and (e). Table 4 demonstrates the improvements in performance figures obtained for the proposed approach on STARE database when compared to existing approaches.

6. Conclusion

Matched filter is well known in retina blood vessel segmentation. Since the widths of the vessels are varying across the image, matched filter with single scale does not provide acceptable performance figures. The proposed approach makes use of two matched filters. Particle swarm optimization based parameter selection is employed for selecting the right values of parameters of the multiscale matched filter. The approach is tested on DRIVE and STARE databases to demonstrate the performance advantages over existing approaches. A sensitivity of 71.32%, specificity of 98.66% and accuracy of 96.33% are obtained on DRIVE database, and a sensitivity of 71.72%, specificity of 96.87% and accuracy of 95% are obtained on STARE database. Results demonstrate that the multiscale matched filter works better than single scale matched filter for vessel segmentation. Future work proposes to introduce vessel morphology to improve the vessel segmentation results for achieving improved performances.

References

- [1] Mitchell Paul, Leung Harry, Wang Jie Jin, Rochtchina Elena, Lee Anne J, Wong Tien Y, Klein Ronald. Retinal vessel diameter and open-angle glaucoma: the blue mountains eye study. *Ophthalmology* 2005;112(2):245–50.
- [2] Ciulla Thomas A, Amador Armando G, Zinman Bernard. Diabetic retinopathy and diabetic macular edema pathophysiology, screening, and novel therapies. *Diabetes Care* 2003;26(9):2653–64.
- [3] Giancardo Luca, Meriaudeau Fabrice, Karnowski Thomas P, Li Yaquin, Tobin Kenneth W, Chaum Edward. Automatic retina exudates segmentation without a manually labelled training set. In: *Biomedical imaging: from nano to macro*, 2011 IEEE international symposium on, IEEE; 2011. p. 1396–1400.
- [4] Sreejini KS, Govindan VK. Severity grading of DME from retina images: a combination of PSO and FCM with bayes classifier. *Int J Comput Appl* November 2013;81(16):11–7.
- [5] Sreejini KS, Govindan VK. Automatic grading of severity of diabetic macular edema using color fundus images. In: *Advances in computing and communications (ICACC)*, 2013 third international conference on, IEEE; 2013. p. 177–180.
- [6] Wasif Reza Ahmed, Eswaran Chantra, Dimiyati Kaharudin. Diagnosis of diabetic retinopathy: automatic extraction of optic disc and exudates from retinal images using marker-controlled watershed transformation. *J Med Syst* 2011;35(6):1491–501.
- [7] Leung Harry, Wang Jie Jin, Rochtchina Elena, Wong Tien Y, Klein Ronald, Mitchell Paul. Impact of current and past blood pressure on retinal arteriolar diameter in an older population. *J Hypertension* 2004;22(8):1543–9.
- [8] Kanski Jack J. *Clinical ophthalmology: a systematic approach*. Boston, Massachusetts: Butterworth Heinemann; 2007. p. 629.
- [9] Niemeijer M, Staal JJ, Ginneken Bv, Loog M, Abramoff MD. Drive: digital retinal images for vessel extraction; 2004. WebLink: <http://www.isi.uu.nl/Research/Databases/DRIVE/>.
- [10] Gonzales Rafael C, Woods Richard E. *Digital image processing*. Addison-Wesley; 1993.
- [11] Zana Frederic, Klein J-C. Segmentation of vessel-like patterns using mathematical morphology and curvature evaluation. *Image Process, IEEE Trans* 2001;10(7):1010–9.
- [12] Fraz Muhammad Moazam, Barman SA, Remagnino Paolo, Hoppe Andreas, Basit Abdul, Uyyanonvara Bunyarit, Rudnicka Alicja R, Owen Christopher G. An approach to localize the retinal blood vessels using bit planes and centerline detection. *Comput Methods Prog Biomed* 2012;108(2):600–16.
- [13] Vlachos Marios, Dermatas Evangelos. Multi-scale retina vessel segmentation using line tracking. *Comput Med Imag Graph* 2010;34(3):213–27.
- [14] Staal Joes, Abramoff Michael D, Niemeijer Meindert, Viergever Max A, van Ginneken Bram. Ridge-based vessel segmentation in color images of the retina. *Med Imag, IEEE Trans* 2004;23(4):501–9, WebLink: <http://www.ces.clemson.edu/~ahoover/stare/>.
- [15] Kande Giri Babu, Venkata Subbaiah P, Savithri T Satya. Unsupervised fuzzy based vessel segmentation in pathological digital fundus images. *J Med Syst* 2010;4(5):849–58.
- [16] Chaudhuri Subhasis, Chatterjee Shankar, Katz Norman, Nelson Mark, Goldbaum Michael. Detection of blood vessels in retinal images using two-dimensional matched filters. *IEEE Trans Med Imag* 1989;8(3):263–9.
- [17] Yao Chang, Chen Hou-jin. Automated retinal blood vessels segmentation based on simplified PCNN and fast 2D-otsu algorithm. *J Central South Univ Technol* 2009;16:640–6.
- [18] Otsu Nobuyuki. A threshold selection method from gray level histograms. *Automatica* 1975;11(285–296):23–7.
- [19] Cinsdikici MG, Aydin D. Detection of blood vessels in ophthalmoscope images using MF/ant (matched filter/ant colony) algorithm. *Comput Methods Prog Biomed* 2009;96(2):85–95.
- [20] Zhang Bob, Zhang Lin, Zhang Lei, Karray Fakhri. Retinal vessel extraction by matched filter with first order derivative of gaussian. *Comput Biol Med* 2010;40(4):438–45.
- [21] Al-Rawi Mohammed, Qutaishat Munib, Arrar Mohammed. An improved matched filter for blood vessel detection of digital retinal images. *Comput Biol Med* 2007;37(2):262–7.
- [22] Al-Rawi Mohammed, Karajeh Huda. Genetic algorithm matched filter optimization for automated detection of blood vessels from digital retinal images. *Comput Methods Prog Biomed* 2007;87(3):248–53.
- [23] Zolfagharnasab Hooshier, Naghsh-Nilchi Ahmad Reza. Cauchy based matched filter for retinal vessels detection. *J Med Signals Sens* 2014;4(1):1.
- [24] Li Qin, You Jane, Zhang David. Vessel segmentation and width estimation in retinal images using multiscale production of matched filter responses. *Expert Syst Appl* 2012;39(9):7600–10.
- [25] Kennedy James, Eberhart Russell. Particle swarm optimization. In: *Proceedings of 1995 IEEE international conference on neural networks*; 1995. p. 1942–8.
- [26] Hoover Adam, Kouznetsova Valentina, Goldbaum Michael. Locating blood vessels in retinal images by piecewise threshold probing of a matched filter response. *Med Imag, IEEE Trans* 2000;19(3):203–10.
- [27] Soares Joao VB, Leandro Jorge JG, Cesar Roberto M, Jelinek Herbert F, Cree Michael J. Retinal vessel segmentation using the 2-D Gabor wavelet and supervised classification. *Med Imag, IEEE Trans* 2006;25(9):1214–22.
- [28] You Xinge, Peng Qinmu, Yuan Yuan, Cheung Yiu-ming, Lei Jiajia. Segmentation of retinal blood vessels using the radial projection and semi-supervised approach. *Pattern Recogn* 2011;44(10):2314–24.
- [29] Martinez-Perez M Elena, Hughes Alun D, Thom Simon A, Bharath Anil A, Parker Kim H. Segmentation of blood vessels from red-free and fluorescein retinal images. *Med Image Anal* 2007;11(1):47–61.
- [30] Perez MEM, Hughes Alun D, Thorn SA, Parker Kim H. Improvement of a retinal blood vessel segmentation method using the insight segmentation and registration toolkit (ITK). In: *Engineering in Medicine and Biology Society, 2007. EMBS 2007. 29th Annual international conference of the IEEE, IEEE*; 2007. p. 892–5.
- [31] Martinez-Perez, Hughes Alun D, Stanton Alice V, Thom Simon A, Bharath Anil A, Parker Kim H. Retinal blood vessel segmentation by means of scale-space analysis and region growing. In: *Medical image computing and computer-assisted intervention, MICCAI99*, Springer; 1999. p. 90–7.
- [32] Miri Mohammad Saleh, Mahloojifar Ali. Retinal image analysis using curvelet transform and multistructure elements morphology by reconstruction. *Biomed Eng, IEEE Trans* 2011;58(5):1183–92.